GEOPHYSICAL RESEARCH LETTERS, VOL. 35, L10202, doi:10.1029/2008GL033538, 2008

Effect of obliteration on crater-count chronologies for Martian surfaces

Matthew R. Smith,[1] Alan R. Gillespie,[1] and David R. Montgomery[1]

Received 5 February 2008; revised 17 March 2008; accepted 28 March 2008; published 29 May 2008.

[1] The density of impact craters calibrated against lunar data is currently the only quantitative measure of surface age for terrestrial planetary surfaces. Unlike the Moon, however, Mars has been weathered and eroded, obliterating some small (<10 km diameter) craters, a phenomenon addressed in the Mariner/Viking days of Mars exploration but commonly overlooked in recent studies. We present a quantitative model that extends this earlier work to assess the effect of erosion and infilling on surface ages inferred from crater-frequency distributions. Our work affirms that small-crater size distributions can be interpreted quantitatively in terms of effects of erosion and crater infilling at rates comparable to those reported for Mars. A reanalysis of prior studies indicates that low to moderate long-term rates of erosion and crater infilling can mask an ancient age and result in small-crater populations similar to those offered as evidence for young and geologically significant surface activity. **Citation:** Smith, M. R., A. R. Gillespie, and D. R. Montgomery (2008), Effect of obliteration on crater-count chronologies for Martian surfaces, *Geophys. Res. Lett.*, *35*, L10202, doi:10.1029/2008GL033538.

1. Introduction

[2] The loss of Martian impact craters through infilling and erosion of the surrounding plains has been predicted [*Öpik*, 1966; *Hartmann*, 1966], modeled [*Chapman et al.*, 1969; *Hartmann*, 1971; *Craddock and Maxwell*, 1990] and observed [e.g., *Carr*, 1992]. As a reminder that, due to crater obliteration, the apparent age of a surface expressed in its crater abundance may be less than the age of the surficial deposits, *Hartmann* [1966] introduced the term "crater retention age."

[3] Crater-frequency distributions were originally estimated only for large craters on extensive surfaces because of limitations of Mariner image resolution. They remain the only basis for numerical dating of Martian surfaces, and their use continues to be refined to include smaller craters [*Hartmann and Neukum*, 2001; *Hartmann*, 2005] as improvements in image resolution allow. These smaller craters are more quickly obliterated. Nevertheless, the increased effect on the crater-frequency curves previously described and modeled by *Chapman et al.* [1969] and *Hartmann* [1971] have not been considered in many recent crater-dating studies.

[4] Recent images from high-resolution satellite-based cameras such as the Mars Orbiter Camera (MOC) and the Thermal Emissivity Imaging Spectrometer (THEMIS) have identified many small, geologically distinct units, some of which may hold important implications for the geological and climatic history of Mars [e.g., *Malin and Edgett*, 2001; *Quantin et al.*, 2004; *Hartmann*, 2005]. Some of these units, such as the light-toned layered deposits (LLD), are more erodable than the rest of the Martian surface [*Malin and Edgett*, 2001] and may not retain small craters over geologic time. Here we build upon early attempts to account for rates of crater obliteration on crater-frequency distributions quantitatively, by modeling its effect on inferred surface ages over the full size range of craters observable from orbit.

2. Methods

[5] Our model is based on an equation that balances steady production (no. craters a^{-1}) with constant-rate obliteration (% craters a^{-1}). It is commonly used to model populations of radionuclides produced by cosmic-ray exposure:

$$N(t) = \frac{p}{\lambda}\left(1 - e^{-\lambda t}\right). \tag{1}$$

N is the abundance of the measured craters at time t, p = crater production rate (no. craters a^{-1}) and λ = crater-loss function (a^{-1}), itself a function of the combined rates of erosion and infilling, β (nm a^{-1}). N, p, and λ all vary with crater diameter (d).

[6] The production rate is taken to be constant for the last 3.5 Ga. It is calculated as the abundance of craters as a function of diameter on a 3.5 Ga Martian surface (derived as best-fit functions through data given by *Hartmann* [2005]) divided by that amount of time, giving the number of craters of a given diameter (km) per Ga:

$$p(d) = 0.29 \cdot \begin{cases} 0.0035(0.13\ln(d) + 0.83)/d^{3.3} & d > 0.001 \textit{ and } d < 1.4 \\ 10^{-1.8\log(d) - 2.59} & d \geq 1.4 \textit{ and } d \leq 48.1 \\ 10^{-2.2\log(d) - 1.89} & d > 48.1 \end{cases} . \tag{2}$$

Neukum et al. [2001] established an empirical equation describing the time dependence of the lunar cratering rate for craters >1 km which *Hartmann* [2005] applied to Mars for all crater diameters as:

$$N_{D>1\mathrm{km}} = \left(5.44 \cdot 10^{-14}\right)\left(e^{6.93t} - 1\right) + \left(8.38 \cdot 10^{-4}\right)t. \tag{3}$$

Comparing their assumption with ours that $\partial p/\partial t = 0$, we calculate an uncertainty in our production function of 1.6, which is less than the factor of 2–3 uncertainty introduced by assigning the lunar cratering rate to Mars [*Hartmann*, 2005].

[1] Department of Earth and Space Sciences, University of Washington, Seattle, Washington, USA.

0094-8276/08/2008GL033538$05.00

[7] Crater obliteration occurs as the crater relief, defined as crater depth (z), is lowered to zero by erosion of the crater rim and surrounding plains together with deposition of colluvium and wind-blown silt/sand within the crater [*Hartmann*, 1971; *Golombek et al.*, 2006a]. Local obliterative phenomena, such as Martian basalt flows, act differently to remove craters and have been shown to affect the shape of the crater-frequency curve uniquely [*Hartmann et al.*, 1981], but are not considered here.

[8] If we assume that the crater population is wholly comprised of primary craters (formed from extra-planetary impact), we may treat the loss of craters simply. The depth $z(d)$ of fresh primary craters has been estimated empirically from satellite observations by *Pike* [1980]: for $d < 5.8$ km, $z = 0.2 \cdot d_p$, and for $d \geq 5.8$ km, a best-fit function through the data provided yields $z = 0.42 \cdot \ln(d) - 0.01$. Adopting the above functions, the resultant formula for the crater-loss function, λ, is:

$$\lambda = \frac{\beta}{1000\xi}; \quad \xi = \begin{cases} 0.2 \cdot d_p & d < 5.8 \\ 0.42 \cdot \ln(d) - 0.01 & d \geq 5.8 \end{cases}. \tag{4}$$

The factor of 1000 is required to convert β to units of km Ga^{-1} for model input.

[9] The final equation for N is thus:

$$N = \frac{1000\xi p(d)}{\beta}\left(1 - e^{-\beta t/(1000\xi)}\right); \quad \xi = \begin{cases} 0.2 \cdot d_p & d < 5.8 \\ 0.42 \cdot \ln(d) - 0.01 & d \geq 5.8 \end{cases}. \tag{5}$$

[10] On Mars, a majority of small craters are assumed to be secondaries, formed from the fallback of ejecta [*McEwen et al.*, 2005], not included equation (5). We therefore modified equation (5) to incorporate one simplistic model of secondary cratering. We apply a mixing ratio of primaries and secondaries from the modeling work of *McEwen et al.* [2005], who assumed their size-frequency distributions as $N = k \cdot d^{-b}$ (k is related to cumulative crater density N; b = slope of the function in log-log space). For primary craters $b_p \approx 2$ [*Wilhelms*, 1987], and for secondaries $b_s \approx 4 \pm 1$ [*McEwen et al.*, 2005]. To determine the values for k, *McEwen et al.* [2005] used another model-derived parameter, d_c, the diameter for which $N_p = N_s$. This value varies with surface age t, so we adopted the median value d_c = 350 m for surfaces with ages near the Hesperian-Amazonian boundary. Therefore, our production functions are:

$$N_p = k_p d^{-2}. \tag{6}$$

$$N_s = 0.1225 k_p d^{-4}. \tag{7}$$

[11] And the proportion of secondary craters in the population is:

$$\frac{N_s}{N_s + N_p} = \Pi_s = \frac{0.1225}{0.1225 + d^2}. \tag{8}$$

McEwen et al. [2005] also derive a value for the diameter at which $N_p = 10 \cdot N_s$, taken as the upper limit for secondary craters (above which $N_s = 0$). This value is also time-dependent, so we assumed a value derived by *McEwen et al.* [2005], N_p = 1.2 km, which correlates in time with the value for d_c.

[12] From empirical studies of secondary craters, $z = \sim 0.1 d_s$ [*Pike and Wilhelms*, 1978; *McEwen et al.*, 2005], half as deep as for a primary crater of the same diameter. In order to account for easier obliteration of the shallow secondaries in our model, we introduce a multiplicative factor $(1 + \Pi_s)$ into our original crater-decay function, which otherwise assumes all small craters are primaries. This results in a new function for λ:

$$\lambda = \frac{\psi\beta}{1000\xi}; \quad \psi = \begin{cases} 1 + \prod_s & d < 1.2 \\ 0 & d \geq 1.2 \end{cases}; \quad \xi = \begin{cases} 0.2d & d < 5.8 \\ 0.42\ln(d) - 0.01 & d \geq 5.8 \end{cases}. \tag{9}$$

[13] The final equation for N in our modified model is given as:

$$N = \frac{1000}{\psi\beta} p(d)\xi\left(1 - e^{-\frac{\psi\beta t}{1000\xi}}\right). \tag{10}$$

[14] The influence of secondary cratering is controversial [*McEwen et al.*, 2005; *Hartmann*, 2007], specifically its impact on the Hartmann Production Function (HPF), upon which our model is based. Deviations from the HPF have been proposed to result from: (1) spatial heterogeneity of secondary production with local enrichments near large primary craters and associated "rays" and (2) greater production of secondaries on Mars than on the Moon [*McEwen et al.*, 2005]. Both deviations would increase the number of small craters on a given landform, in which case our model results may be taken as lower limits for β. While we regard equation (10) as an improvement on equation (5), further refinements will be necessary when the role of secondary cratering is better understood.

3. Model Validation

[15] The model was tested by calculating values of the crater obliteration rate, β, for 1 km^2 areas at the MER landing sites in Gusev crater and Meridiani Planum from crater abundances and comparing them with ground-based estimates of erosion rates [*Golombek et al.*, 2006a]. To estimate optimal values for β, our obliteration model crater-frequency curves were fit, using weighted least-squares regression in Maple, to independent crater counts [*Hartmann*, 2005; *Golombek et al.*, 2006b] (Figure 1). The type of crater population (primary or secondary) was assigned sensu *Grant et al.* [2006]. For the landing sites, erosion rates were converted to β for comparison with model-derived results, assuming that all eroded material was deposited within craters [*Golombek et al.*, 2006a]. The independently measured *N/d* values, converted into area and summed, were used to calculate the fractional area occupied by craters at each landing site. We then calculated the volume of eroded material per km^2 at both sites, assuming that

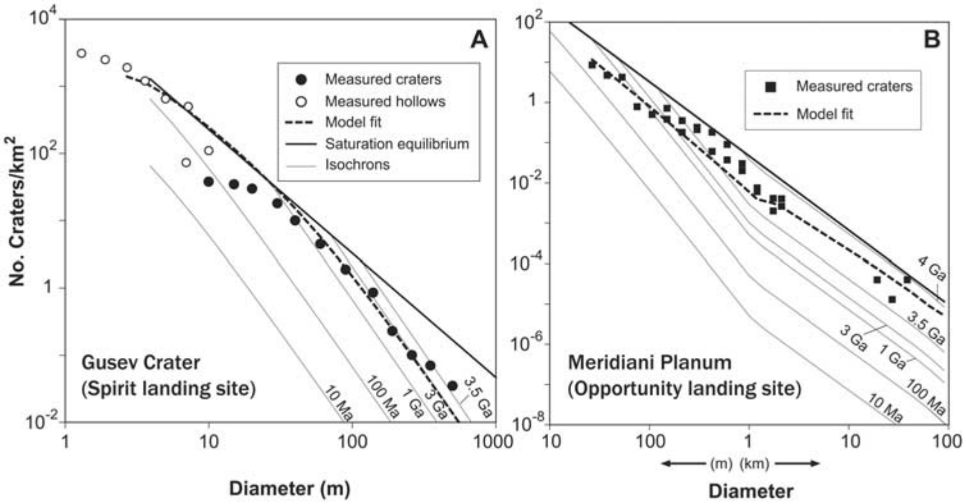

Figure 1. Model fits for crater-frequency counts performed at MER landing sites by (a) *Golombek et al.* [2006b] and (b) *Hartmann* [2005]. In Figure 1a, isochrons and model fits do not extend below 4 m. Below this diameter, atmospheric loss of impactors may be substantial [*Hartmann*, 2005] and available data on crater abundance is limited by image resolution.

erosion was confined to non-cratered areas. The volume of eroded material was divided by crater-occupied surface area, then divided by deposit age to determine a deposition rate which, summed with the erosion rate, yields β. Values for all parameters are given in Table 1.

[16] Although t is also solved for in the model, it is highly sensitive to initial conditions. More precise estimates of the modeled surface age are made by examining the relationship of the modeled isochron to the established isochrons at very large diameters (128 km), for which the effect of obliteration is minimal.

[17] In the Gusev cratered plains, two populations of circular depressions, craters and hollows, are identified and kept distinct in Figure 1a, although they are combined in our model input since hollows are taken to be partially filled craters [*Golombek et al.*, 2006b]. Ground observations suggest that the crater population is entirely secondaries [*Grant et al.*, 2006]. Our model result gives the best-fit value of β in Gusev Crater as 4.72 ± 2.58 nm a^{-1} (Figure 1a), compared to ground-based observations of β between 0.08–5.03 nm a^{-1}, which encompasses our model-derived value.

[18] Meridiani Planum shows evidence of higher erosion rates than the Gusev plains, owing to its structurally weak sulfate-rich composition [*Arvidson et al.*, 2006]. Analysis of depth/diameter ratios of Meridiani craters indicates that they are mostly primary [*Grant et al.*, 2006]. Observed β values fall between 13.5–108.1 nm a^{-1}. The model β value derived from fitting the crater-frequency distribution curve is 27.2 ± 6.0 nm a^{-1} (Figure 1b), which falls within the range of calculated values.

4. Effect of Crater Obliteration on Crater-Frequency Curves

[19] Reported erosion and deposition rates on Mars range from 10^{-2} to 10^{5} nm a^{-1} (given in the auxiliary material[1]). The highest rates (>1000 nm a^{-1}) may pertain only to the Noachian era (>3.7 Ga [*Hartmann and Neukum*, 2001]). The responses of crater-frequency curves to this observed range of β were calculated for two surfaces (100 Ma and 3 Ga old) using our model (Figure 2). The qualitative results for this exercise hold for both the primary-only and the primary-secondary models. Quantitative results are discussed for the primary-only case, with the modified-model results (including secondaries) given in parentheses.

[20] Because obliteration is more efficient for small craters, higher β values produce a more pronounced roll-off of the crater-frequency curve for small craters relative to the predicted isochron for a given surface, as discussed by *Chapman et al.* [1969] and *Hartmann* [1971]. A greater obliteration rate increases the diameter where the curve deviates from its predicted isochron. The effect of obliteration is less for younger surfaces, because erosion and infilling have had less time to affect the surface: the roll-off becomes less pronounced for younger surfaces and the deviation point shifts to smaller diameters. The implications can be seen when dating ancient surfaces (~3 Ga). For β = 100 nm a^{-1} (within the range of values observed at Meridiani Planum), if only small craters (<300 m) are considered the predicted age will be ~2 Ga (2.5 Ga) too young (Figure 2a). If only craters <100 m are considered, apparent surface ages may underestimate the geological age by an order of magnitude. For β = 1000 nm a^{-1}, the

Table 1. Landing Site Parameters for Model Verification

	Crater Cover, %	Surface Age, Ga	Eroded Thickness, m	Equiv. Deposited Thickness, m	β, nm a^{-1}
Gusev Crater	17[a]	~3.5[a]	0.05–3[b]	0.24–14.6	0.08–5.03
Meridiani Planum	20[c,d]	~3.7[b]	10–80[b]	40–320	13.5–108.1

[a]*Golombek et al.* [2006b].
[b]*Golombek et al.* [2006a].
[c]*Hartmann* [2005].
[d]Including craters exhumed from beneath Amazonian surficial basaltic sand layer.

[1]Auxiliary materials are available in the HTML. doi:10.1029/2008GL033538.

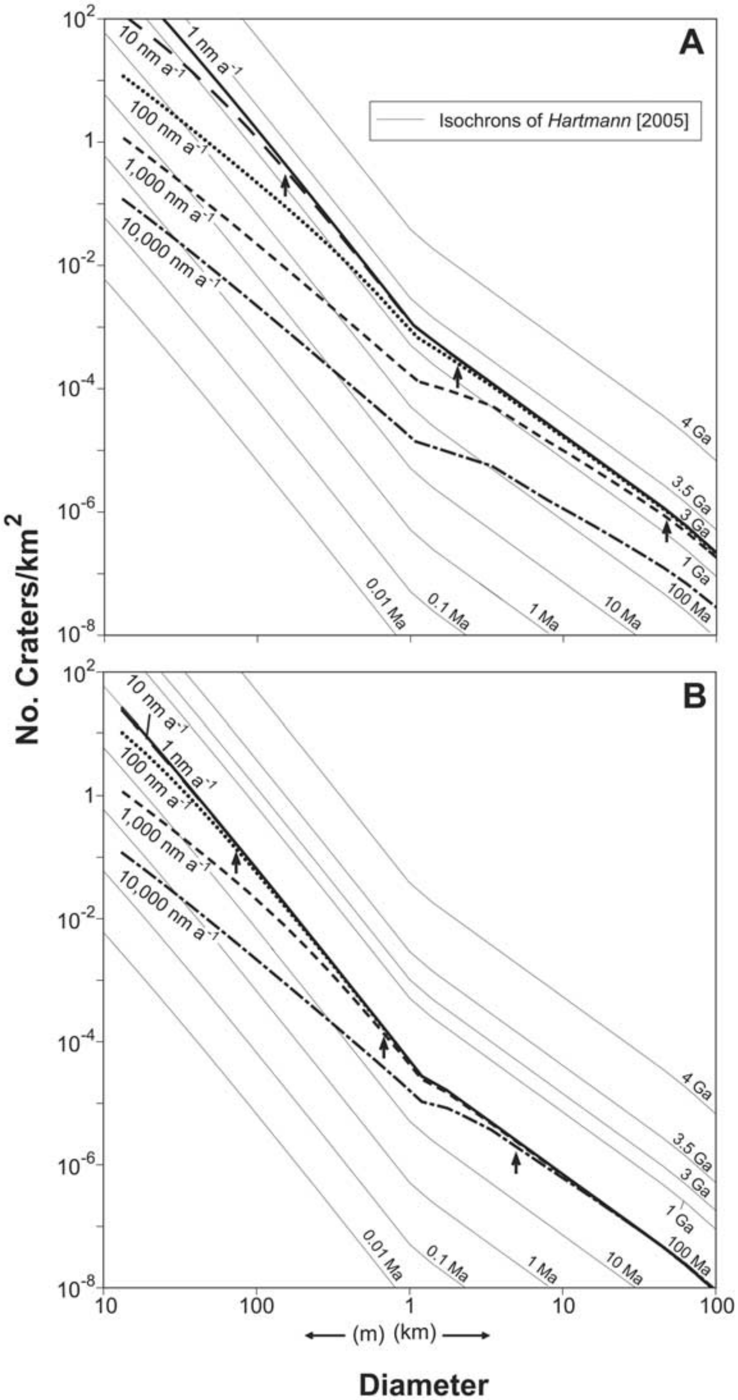

Figure 2. Response of crater-frequency curve to several constant obliteration (combined erosion and deposition) rates, β, on surfaces with ages (a) 3 Ga and (b) 100 Ma, assuming only primary cratering. Arrows indicate where associated curve deviates from predicted isochron.

predicted age will be decreased from 3 Ga to ~500 Ma (300 Ma) for preserved craters <1 km in diameter and to ~50 Ma (10 Ma) for preserved craters <100 m in diameter. Although this rate is at the high end of those estimated for Mars, similar rates have been estimated for LLD [*Komatsu et al.*, 1993], which are susceptible to erosion as shown by their wind-sculpted yardangs and strong bench-and-cliff structures [*Malin and Edgett*, 2001]. For younger surfaces, (e.g., 100 Ma), β = 1000 nm a^{-1} may reduce the apparent age by 90%, to 10 Ma (95%, 5 Ma). A lower obliteration rate of β = 100 nm a^{-1} affects the curve only at very small crater sizes (<20 m) and reduces the apparent age only to 80–90 Ma (30–40 Ma) (Figure 2b).

5. Reanalysis of Previous Crater-Count Studies

[21] We reanalyzed ages inferred from crater counts in three recent studies that focused on small craters (<1 km) and on surfaces that appeared to be partially eroded: a

landslide in Coprates Chasma [*Quantin et al.*, 2004], a glacier-like tongue east of Hellas Basin and layered sediments in W. Arabia Terra crater [*Hartmann*, 2005]. Unless otherwise noted, the results are calculated using our modified model, which includes secondary craters, to achieve a more accurate portrayal of the likely crater population. Primary-only model results increase the derived β by a factor of ~2.

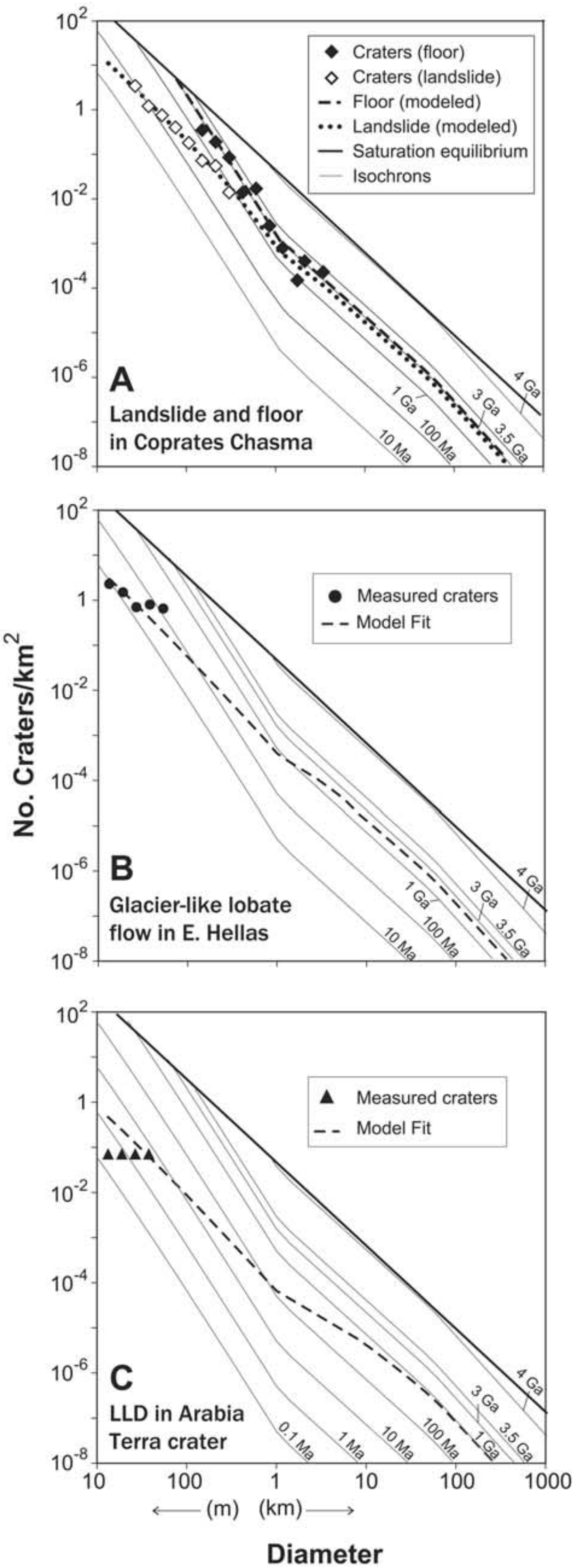

Figure 3. Model fits to prior studies using crater-frequency distributions to date small deposits, assuming a mixed population of primary and secondary craters. Crater counts from (a) *Quantin et al.* [2004] and (b and c) *Hartmann* [2005]. Isochrons and saturation equilibrium line from *Hartmann* [2005].

[22] *Quantin et al.* [2004] measured the crater density on several landslides throughout Valles Marineris to assess the persistence of landsliding and seismicity throughout the history of the canyon system, ~3.5 Ga. Their study identified three types of crater populations: (1) the crater-frequency distribution follows the slope of an isochron and a precise age estimate can be made, (2) the slope of the distribution is shallower than the isochrons and only a minimum age estimate can be constrained by the largest craters on the slide, and (3) the distribution follows an isochron for large craters but shallows for smaller ones. One landslide that was highlighted in their study and said to exemplify the latter type was found in Coprates Chasma and had an estimated age of 400 Ma. The surface of the landslide is extensively "etched," with prevalent scoured pits aligned oblique to the original flow lines. The obliteration model fit to the crater-frequency distribution for the landslide yielded $\beta = 54 \pm 37$ nm a^{-1} (Figure 3a), within the range of values of β reported at Meridiani Planum. Their study argued against substantial erosion on this and other slides, offering as evidence the observation that flow lines with low relief (30 m) are preserved. However, if we assume that erosion accounts for ~20% of β (as observed at the MER landing sites), the total eroded thickness modeled would be ~3–18 m Ga^{-1}, low enough to preserve many fine-scale surface features over geological time. The best-fit model age for the landslide is similar to that obtained for the chasm floor (~3 Ga) if only large-diameter craters with minimal obliteration are considered, illustrating how even intermediate erosion rates would lead to a reduction of the apparent crater age for the landslide by a factor of six.

[23] The tongue-shaped, glacier-like feature located to the east of Hellas Basin (38°S, 113°E), was provisionally identified as a rock glacier. On the basis of its low crater abundance [*Hartmann*, 2005], it has been posited as evidence of recent ice accumulation and flow [*Arfstrom and Hartmann*, 2005] in response to recent Martian obliquity shifts (~5–20 Ma). We applied our model and determined that a value for $\beta = 197 \pm 107$ nm a^{-1} can explain the low crater-counts, without any recent surface-resetting flow event. For large crater diameters, the isochron indicates ages of ~2 Ga, whereas conventional isochrons for small craters indicate ages as much as two orders of magnitude lower (Figure 3b). This fitted value for β is higher than near the rover landing sites, but may be reasonable for an ice-rich deposit affected by sublimation of near-surface ice, erosion of weak and unconsolidated drift, or possibly through viscous relaxation within an ice-rich deposit, as observed on the south polar layered deposits [*Pathare et al.*, 2005].

[24] The third example has been associated with exhumation of an ancient LLD within a crater in W. Arabia

Terra, near 8°N, 353°E [*Malin and Edgett*, 2001]. The age of exhumation was constrained by crater counts and an upper limit was established, from the abundance of the observed craters with the largest diameter, at a few million years [*Hartmann*, 2005]. The exhumation was related to recent Martian obliquity shifts by *Arfstrom and Hartmann* [2005], since the change in obliquity would result in the deposition of ice-rich mantles in mid to low-latitude basins that would shield subjacent surfaces. The sedimentary layers exposed on the floor of the crater have been topographically modified, with strong bench-and-cliff morphology observed across the surface. There are very few craters [*Hartmann*, 2005], and many of these appear to be filled with dark sediment and lack a well-defined rim, indicative of erosion. Using β = 1000 nm a^{-1}, a predicted crater-frequency curve was fit through the abundance of the largest diameter craters to yield model ages $\leq$1 Ga (Figure 3c). Because the evidence for intense post-exhumation surface modification is strong, such ages present a reasonable alternative hypothesis.

[25] For all three studies, our model demonstrated the potential for surface ages much greater than the originally reported ones due to the influence of processes such as eolian erosion and crater infilling. Our model results do not provide unique solutions, but they do effectively broaden both the range of possible surface ages and explanations for the observed crater populations. Although two of these sites yielded model-derived values for β that were higher than those calculated at either rover landing site, the observed surface modification was commensurately greater in these cases.

6. Conclusions

[26] Our findings support the long-articulated, but seldom implemented view that erosion must be accounted for when using crater-counting to ascertain Martian surface ages, especially for small and heavily modified landforms and deposits. For low long-term rates of obliteration ($\leq$10 nm a^{-1}), we find that surface modification has a minimal effect on the calculated surface age, even when only small craters are counted. For higher rates $\geq$50 nm a^{-1}, the change of the calculated surface age can be large, especially when counting only small craters. This sensitivity demonstrates that accurately determining the ages of small landscape elements cannot be done by crater counting without considering infilling and erosion. For readily eroded deposits, especially for small areas with few large craters, apparent ages may be much too low and cannot be constrained to yield unambiguous information about Martian chronology and evolution.

[27] **Acknowledgments.** Comments by W. Hartmann, G. Komatsu, A. McEwen and an anonymous reviewer improved the manuscript.

References

Arfstrom, J., and W. K. Hartmann (2005), Martian flow features, moraine-like ridges, and gullies: Terrestrial analogs and interrelationships, *Icarus*, *174*, 321–335.

Arvidson, R. E., et al. (2006), Nature and origin of the hematite-bearing plains of Terra Meridiani based on analyses of orbital and Mars Exploration rover data sets, *J. Geophys. Res.*, *111*, E12S08, doi:10.1029/2006JE002728.

Carr, M. H. (1992), Post-Noachian erosion rates: Implications for Mars climate, *Lunar Planet. Sci.*, *XXIII*, 205–206.

Chapman, C. R., J. B. Pollack, and C. Sagan (1969), An analysis of the Mariner-4 cratering statistics, *Astronom. J.*, *74*, 1039–1051.

Craddock, R. A., and T. A. Maxwell (1990), Resurfacing of the Martian highlands in the Amenthes and Tyrrhena region, *J. Geophys. Res.*, *95*, 14,265–14,278.

Golombek, M. P., et al. (2006a), Erosion rates at the Mars Exploration Rover landing sites and long-term climate change on Mars, *J. Geophys. Res.*, *111*, E12S10, doi:10.1029/2006JE002754.

Golombek, M. P., et al. (2006b), Geology of the Gusev cratered plains from the Spirit rover transverse, *J. Geophys. Res.*, *111*, E02S07, doi:10.1029/2005JE002503.

Grant, J. A., et al. (2006), Crater gradation in Gusev crater and Meridiani Planum, Mars, *J. Geophys. Res.*, *111*, E02S08, doi:10.1029/2005JE002465.

Hartmann, W. K. (1966), Martian cratering, *Icarus*, *5*, 565–576.

Hartmann, W. K. (1971), Martian cratering III: Theory of crater obliteration, *Icarus*, *15*, 410–428.

Hartmann, W. K. (2005), Martian cratering 8: Isochron refinement and the chronology of Mars, *Icarus*, *174*, 294–320.

Hartmann, W. K. (2007), Martian cratering 9: Toward resolution of the controversy about small craters, *Icarus*, *189*, 274–278.

Hartmann, W. K., and G. Neukum (2001), Cratering chronology and the evolution of Mars, *Space Sci. Rev.*, *96*, 165–194.

Hartmann, W. K., et al. (1981), Chronology of planetary volcanism by comparative studies of planetary cratering, in *Basaltic Volcanism on the Terrestrial Planets*, edited by R. Merrill and R. Ridings, pp. 1050–1127, Pergamon, New York.

Komatsu, G., P. E. Geissler, R. G. Strom, and R. B. Singer (1993), Stratigraphy and erosional landforms of layered deposits in Valles Marineris, Mars, *J. Geophys. Res.*, *98*, 11,105–11,121.

Malin, M. C., and K. S. Edgett (2001), Sedimentary rocks of early Mars, *Science*, *290*, 1927–1937.

McEwen, A. S., et al. (2005), The rayed crater Zunil and interpretations of small impact craters on Mars, *Icarus*, *176*, 351–381.

Neukum, G., et al. (2001), Mars/Moon cratering rate ratio estimates, in *Chronology and Evolution of Mars*, edited by R. Kallenbach, W. K. Hartmann, and J. Geiss, pp. 87–104, Springer, New York.

Öpik, E. J. (1966), The Martian surface, *Science*, *153*, 255–265.

Pathare, A. V., D. A. Paige, and E. Turtle (2005), Viscous relaxation of craters within the Martian south polar layered deposits, *Icarus*, *174*, 396–418.

Pike, R. J. (1980), Control of crater morphology by gravity and target type: Mars, Earth, Moon, *Proc. Lunar Planet. Sci. Conf.*, *XIth*, 2159–2189.

Pike, R. J., and D. E. Wilhelms (1978), Secondary-impact craters on the Moon: Topographic form and geologic process, *Proc. Lunar Planet. Sci. Conf.*, *IXth*, 907–909.

Quantin, C., P. Allemand, N. Mangold, and C. Delacourt (2004), Ages of Valles Marineris (Mars) landslides and implications for canyon history, *Icarus*, *172*, 555–572.

Wilhelms, D. E. (1987), The geologic history of the Moon, *U.S. Geol. Surv. Prof. Pap.*, *1840*, 302 pp.

A. R. Gillespie, D. R. Montgomery, and M. R. Smith, Department of Earth and Space Sciences, University of Washington, Box 351310, 4000 15th Avenue NE, Seattle, WA 98195-1310, USA. (matthers@u.washington.edu)